

# Activity and N<sub>2</sub> Selectivity of Sol–Gel Prepared Pt/Alumina Catalysts for Selective NO<sub>x</sub> Reduction

Erol Seker and Erdogan Gulari<sup>1</sup>

*Chemical Engineering Department, University of Michigan, Ann Arbor, Michigan 48109-2136*

Received May 21, 1999; revised May 31, 2000; accepted June 5, 2000

We prepared 1 and 2 wt% Pt/Al<sub>2</sub>O<sub>3</sub> catalysts by a single-step sol–gel process and tested their activity and N<sub>2</sub> selectivity for NO<sub>x</sub> reduction with propene. Our results show that when compared to the impregnation catalysts, the single-step sol–gel catalysts have superior N<sub>2</sub> selectivity both in terms of percentage of NO converted to N<sub>2</sub> (~70% or greater) and comparable activity. All of the catalysts tested show a minimum in N<sub>2</sub> selectivity at the point of maximum NO<sub>x</sub> conversion. Both the value of the minimum selectivity and the NO<sub>x</sub> conversion are functions of oxygen concentration in the feed. The N<sub>2</sub> selectivity at peak conversion exhibits a minimum at ~6.8% O<sub>2</sub>. Increasing the feed oxygen concentration beyond 6.8% has many beneficial effects including broadening of the temperature window, suppression of NO<sub>2</sub> formation and increasing the N<sub>2</sub> selectivity without significantly changing the maximum NO<sub>x</sub> conversion. The sol–gel catalysts show remarkable robustness after exposure to high temperatures, SO<sub>2</sub>, and long time exposure to reactants.

© 2000 Academic Press

**Key Words:** selective NO reduction; platinum/alumina catalysts; sol–gel preparation; propene; N<sub>2</sub> selectivity.

## I. INTRODUCTION

Diesel engines are the main mobile sources of NO<sub>x</sub> emissions. For these vehicles, three-way catalysts are useless due to net-oxidizing condition of their exhaust streams. Hence, NO<sub>x</sub> removal from a lean exhaust stream by selective catalytic reduction with a hydrocarbon has been an active research area since it was demonstrated that hydrocarbons could be used as reductants (1–3). Thereafter, many catalyst formulations have been proposed and can be roughly grouped into zeolite supported and metal oxide supported catalysts. For zeolite-supported catalysts, ZSM-5 is a common choice as a support to disperse a transition metal as active site (4–6). Even though it has been shown that ZSM-5 based catalysts are active for NO<sub>x</sub> reduction, they do not have stability at high temperatures in the presence of water vapor (7, 8). Supported platinum metal based catalyst have shown the highest activities at the lowest temperatures

for selective NO<sub>x</sub> reduction (9–12). Among the metal oxide supports used for supporting platinum, alumina is the support of choice because of its stability and high surface area. However, platinum-based catalysts have two major limitations, high selectivity to N<sub>2</sub>O and the narrow temperature window of activity (1, 10, 13). Perhaps more than the narrow activity window, selectivity to N<sub>2</sub>O is particularly undesirable because N<sub>2</sub>O is approximately 200 times worse than CO<sub>2</sub> as a greenhouse gas and in the upper atmosphere it interferes with the ozone cycle. For most Pt/alumina catalysts the selectivity to N<sub>2</sub>O can be as high as 70% (12, 13) when propene is used as the reductant. Burch and Ottery (13) have reported that by changing the hydrocarbon, selectivity to N<sub>2</sub> can be increased significantly. Recently, we have demonstrated that the method of preparation can change the activity and selectivity of alumina supported metal catalysts for selective reduction of NO<sub>x</sub> with hydrocarbons (14, 15). In this manuscript we report more extensive selectivity and activity results obtained in selective reduction of NO<sub>x</sub> with propene using single-step sol–gel prepared Pt/Alumina catalysts.

## II. EXPERIMENTAL DETAILS

### A. Catalyst Preparation

We used aluminum *tri-sec*-butoxide to make alumina support and hexachloroplatinic acid for Pt loading. For a desired Pt loading, a necessary amount of hexachloroplatinic acid and aluminum *tri-sec*-butoxide in the presence of excess water and a solvent were mixed in an orderly manner as described previously (15). The resulting gels were dried at 100°C for 12 h to remove the solvent and water followed by calcining at 600°C for 24 h. These catalysts were used in catalytic testing without further pretreatment. Impregnation prepared catalysts were prepared using the sol–gel made alumina (prepared as described above) and a commercial  $\delta$ -alumina (C-alumina from Degussa) and were calcined using the same procedure as the single-step sol–gel catalysts.

<sup>1</sup> To whom correspondence should be addressed. E-mail: [gulari@engin.umich.edu](mailto:gulari@engin.umich.edu).

### B. Catalyst Testing

All catalysts were tested by using a quartz U-tube (i.d. 3 mm) flow reactor. The catalyst, 0.036 g, was put between two quartz wool plugs after grinding and sieving to 120–180 mesh size. The total flow rate was kept constant at 72 ml/min. The reactant gas mixture was blended by using four independent mass flow controllers to give 750 ppm NO and 10 ppm NO<sub>2</sub> (coming from the NO cylinder), 762 ppm propene, 1–13% O<sub>2</sub>, 2.6% H<sub>2</sub>O (when used) and He as balance. The reactor outlet stream was analyzed by using a Thermo Environmental 42CHL NO<sub>x</sub> Chemiluminescence Analyzer to determine unreacted NO<sub>x</sub> and also by FTIR with a 10-cm path length gas cell for quantitative determination of CO<sub>2</sub>, CO, and N<sub>2</sub>O. In general, the activity measurements were reproducible within  $\pm 2\%$  and the N<sub>2</sub>O selectivity measurements were accurate to  $\sim 5$  ppm resulting in an error bar of  $\pm 2\%$  in N<sub>2</sub> selectivity at 50% NO<sub>x</sub> conversion. The determination of the peak conversion temperature has an error of  $\pm 5^\circ\text{C}$  due to oscillations seen with the impregnation catalysts.

### C. Catalyst Characterization

We characterized the catalysts by XRD to determine approximate crystallite size and phases present. BET and TEM were used to determine the metal crystallite size and distribution. CO chemisorption was used to determine Pt dispersion. XPS was tried to obtain electronic state information about alumina and oxygen but was not useful for platinum because of the overlap between the Pt and Al peaks.

## III. RESULTS

### A. Effect of Preparation Method and Loading on Activity and Selectivity

One major difference we noticed immediately between the single-step sol-gel catalysts and the impregnation made catalysts was their initial activity: single-step sol-gel catalysts (SG) were active immediately after preparation. The impregnation catalysts were not active and had to be reduced with flowing H<sub>2</sub> at 500°C for 5 h prior to catalytic testing to activate them. We also had to leave them on stream overnight to stabilize their performance. The difference may be due to the hydrocarbon assisted removal of residual chlorine from the sol-gel catalysts during the calcination period. Since the metallic Pt crystallites of the single-step sol-gel catalysts appear to be formed before the gelation of the support it is also possible that the chlorine is not associated with platinum in these catalysts at all. The conversion level as well as the selectivity observed with the impregnation catalysts showed long lived periodic and random oscillations with amplitudes of as much as  $\pm 10\%$  in the neighborhood of peak conversion temperature. In

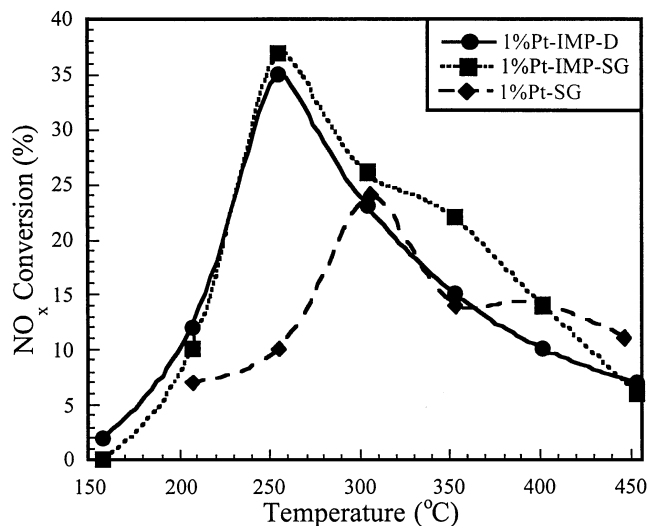


FIG. 1. A comparison of the NO<sub>x</sub> reduction activity of 1 wt% Pt/alumina catalysts. Conditions: 0.036 g catalyst, 750 ppm of NO 10 ppm NO<sub>2</sub>, 762 ppm C<sub>3</sub>H<sub>6</sub>, 2.6% H<sub>2</sub>O, 6.8% O<sub>2</sub>, remainder He. Total flow rate 72 ml/min.

contrast, no significant oscillations were observed with the sol-gel catalysts.

Figures 1 and 2 show the effect of preparation method on the NO<sub>x</sub> conversion activity as a function of temperature for 1 and 2% Pt/alumina catalysts, prepared in three different ways: single-step sol-gel (SG), impregnation using sol-gel prepared alumina (IMP-SG), and impregnation using  $\delta$ -alumina (IMP-D). For the 1% Pt catalysts the SG catalyst is the least active and reaches its peak activity of 24% conversion at  $\sim 300^\circ\text{C}$ . The two impregnation catalysts

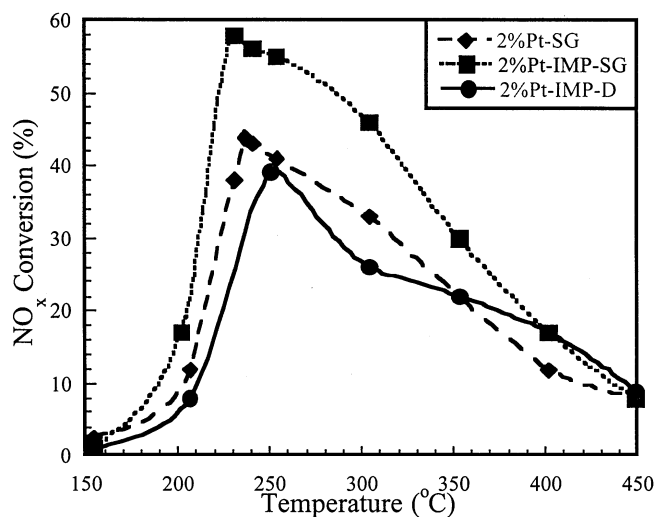


FIG. 2. A comparison of the NO<sub>x</sub> reduction activities of 2 wt% Pt/alumina catalysts. Conditions: 0.036 g catalyst, 750 ppm of NO 10 ppm NO<sub>2</sub>, 762 ppm C<sub>3</sub>H<sub>6</sub>, 2.6% H<sub>2</sub>O, 6.8% O<sub>2</sub>, remainder He. Total flow rate 72 ml/min.

have the same peak activity temperature of 254°C, with peak NO<sub>x</sub> conversions of ~35 and 39% for the IMP-D and IMP-SG catalysts, respectively. In general, the activity of the IMP-SG is higher on the high temperature side of the peak conversion by 3 to 8%. Among the 2% Pt catalysts, the IMP-SG catalyst is the most active, starting at 200°C it becomes highly active and reaches a maximum conversion of 58% at 230°C. The SG catalyst is the next most active and reaches a peak conversion of 46% at 240°C. Commercial  $\delta$ -alumina catalyst (IMP-D) is the least active and reaches a peak conversion of 39% at 250°C. The shapes of the activity versus temperature curves are somewhat different. Interestingly there is very little difference between the activity and selectivity curves of 1 and 2% IMP-D catalysts. They can almost be superimposed within experimental error. In agreement with the findings of Burch and Ottery (13) who reported that N<sub>2</sub> selectivity does not change with either space velocity or Pt loading. In comparison, the SG and IMP-SG catalysts show significant increases in activity due to loading. The data shown in Figs. 1 and 2 were taken in the presence of 2.6% water. If we remove the water, the changes seen are relatively minor: the peak conversions increase by 3–5% and the peak conversion temperatures decrease by ~10°C and the width of the activity curve decreases by ~10–20°C.

Figures 3 and 4 show the N<sub>2</sub> selectivities as a function of temperature under the same conditions of Fig. 1. Common to all the curves is the presence of a minimum in N<sub>2</sub> selectivity at the temperature of maximum NO<sub>x</sub> conversion. Figure 3 shows that the selectivities of the two impregnation catalysts are the same within error. Selectivity of the single-step sol-gel catalyst is much higher than the other

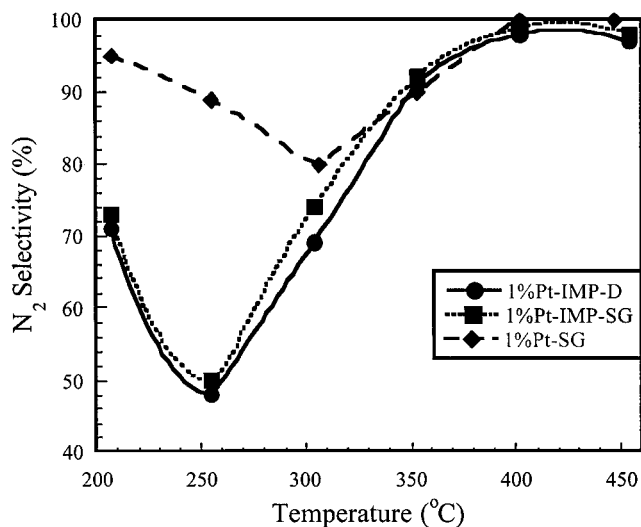


FIG. 3. N<sub>2</sub> selectivities of 1 wt% Pt loading catalysts as a function of temperature. Conditions: 0.036 g catalyst, 750 ppm of NO 10 ppm NO<sub>2</sub>, 762 ppm C<sub>3</sub>H<sub>6</sub>, 2.6% H<sub>2</sub>O, 6.8% O<sub>2</sub>, remainder He. Total flow rate 72 ml/min.

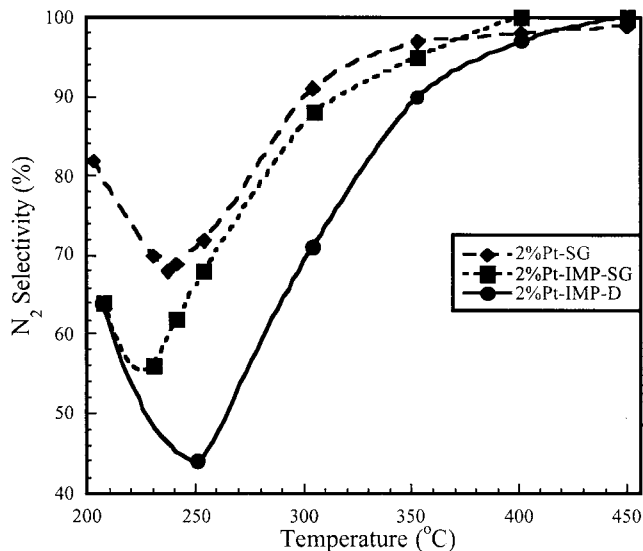


FIG. 4. N<sub>2</sub> selectivities of 2 wt% Pt/alumina catalysts as a function of temperature. Conditions: 0.036 g catalyst, 750 ppm of NO 10 ppm NO<sub>2</sub>, 762 ppm C<sub>3</sub>H<sub>6</sub>, 2.6% H<sub>2</sub>O, 6.8% O<sub>2</sub>, remainder He. Total flow rate 72 ml/min.

two up to 300°C. Above 300°C the selectivities (as well as the activities) of all three catalysts coincide within error. Among the 2% Pt loading catalysts again the sol-gel catalyst is the most selective, having a minimum selectivity of 69% at peak conversion temperature. IMP-SG catalyst has the next highest N<sub>2</sub> selectivity, 56% at the temperature of maximum NO<sub>x</sub> conversion. The IMP-D catalyst has the lowest N<sub>2</sub> selectivity of 42% in agreement with the literature reports (2, 16). Between 250 and 450°C the selectivities of the sol-gel based catalysts are very close, reaching 95% N<sub>2</sub> selectivity at 350°C (for ~32–35% NO<sub>x</sub> conversion).

#### B. Effect of Oxygen Concentration on Activity and Selectivity

We investigated the dependence of activity and selectivity on oxygen concentration in detail for the three 2% Pt catalysts prepared in three different ways. Figure 5 shows the NO<sub>x</sub> conversion activity of the SG catalyst as a function of oxygen concentration in the feed. The general shape of the activity curves for the 2% Pt-IMP-SG and IMP-D catalysts are similar. For the SG catalyst the peak conversion temperature decreases with increasing oxygen concentration, going from ~290°C at 1% O<sub>2</sub> to ~230°C at 13% O<sub>2</sub>. For the IMP-SG catalyst, the peak conversion temperature decreased from 275°C for 1% O<sub>2</sub> to 230°C for 6.8% O<sub>2</sub> and essentially stayed constant at this value for the higher oxygen concentrations. The IMP-D catalyst also exhibited a decrease in the temperature of peak conversion, going from 260°C at 3% O<sub>2</sub> to 230°C at 10% O<sub>2</sub>. Figure 6 shows the dependence of peak NO<sub>x</sub> conversion on the oxygen concentration in the feed for all three catalysts. The peak

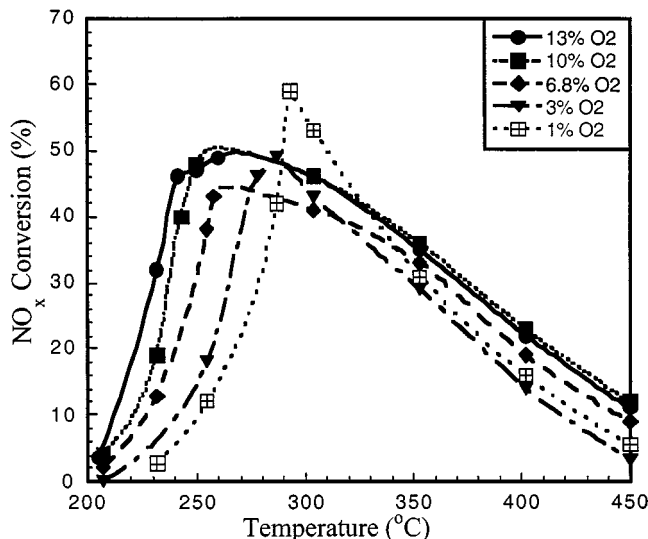


FIG. 5. Oxygen concentration dependence of the NO<sub>x</sub> conversion over 2 wt% Pt single-step sol-gel, SG, catalyst. Conditions: 0.036 g catalyst, 750 ppm of NO 10 ppm NO<sub>2</sub>, 762 ppm C<sub>3</sub>H<sub>6</sub>, 2.6% H<sub>2</sub>O, varying oxygen concentration, remainder He. Total flow rate 72 ml/min.

conversion for the SG catalyst starts at 60% for 1% O<sub>2</sub> decreasing to a minimum of 45% at 6.8% O<sub>2</sub> and then increases with increasing oxygen concentration reaching 49% at 10% O<sub>2</sub>. Peak NO<sub>x</sub> conversion of the IMP-SG catalyst decreases continuously with increasing oxygen concentration starting at 64% NO<sub>x</sub> conversion for 1% O<sub>2</sub> and decreasing to 45% for 13% O<sub>2</sub>. IMP-D catalyst also exhibits a minimum in conversion of 39% at 6.8% O<sub>2</sub>. The accuracy of our

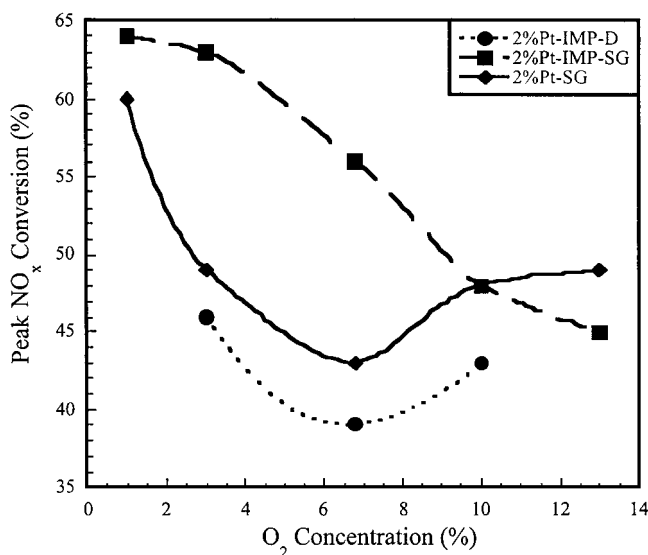


FIG. 6. Oxygen concentration dependence of peak NO<sub>x</sub> conversion activity for all three catalysts. Conditions: 0.036 g catalyst, 750 ppm of NO 10 ppm NO<sub>2</sub>, 762 ppm C<sub>3</sub>H<sub>6</sub>, 2.6% H<sub>2</sub>O, varying oxygen concentration, remainder He. Total flow rate 72 ml/min.

conversion measurements based on repeated experiments is  $\sim \pm 2\%$  thus the changes seen are beyond experimental error.

An important observation we made with all the catalysts has to do with the width of the NO<sub>x</sub> conversion peak versus temperature. Increasing oxygen concentration widens the activity window significantly on the low temperature side slightly on the high temperature side of the conversion peak. The full width at half maximum of NO<sub>x</sub> conversion (FWHM) for the catalysts increases with oxygen concentration in the feed for the three different 2% Pt/alumina catalysts. FWHM goes from a minimum of  $\Delta T \sim 80^\circ\text{C}$  for 1% O<sub>2</sub> to  $\Delta T \sim 180^\circ\text{C}$  for 10% O<sub>2</sub>. For 10% O<sub>2</sub> concentration the catalysts are active from  $\sim 210$  to  $\sim 390^\circ\text{C}$ , covering almost the complete exhaust temperature window for small turbo charged diesel engines (17). The changes seen in the N<sub>2</sub> selectivity of the three catalysts at peak NO<sub>x</sub> conversion as a function of oxygen concentration are also similar as shown in Fig. 7. N<sub>2</sub> selectivity is minimum at  $\sim 6.8\%$  O<sub>2</sub> and increases moderately on both sides of this concentration. The distinct and significant difference between the selectivities of the three catalysts, however, remains at all oxygen concentrations. The SG catalyst selectivity at peak conversion ranges from 68 to 82%, IMP-SG catalyst selectivity is between 56 and 72%, and the IMP-D catalyst selectivity increases from 42 to 52% over a range of 3% O<sub>2</sub> to 10% O<sub>2</sub>.

### C. Conversion and Selectivity under Transient Conditions

We also ran one transient conversion experiment with our 2% Pt sol-gel catalyst and a fully formulated commercial 5% Pt/alumina impregnation catalyst (Ford test catalyst) under almost identical conditions (the sol-gel catalyst

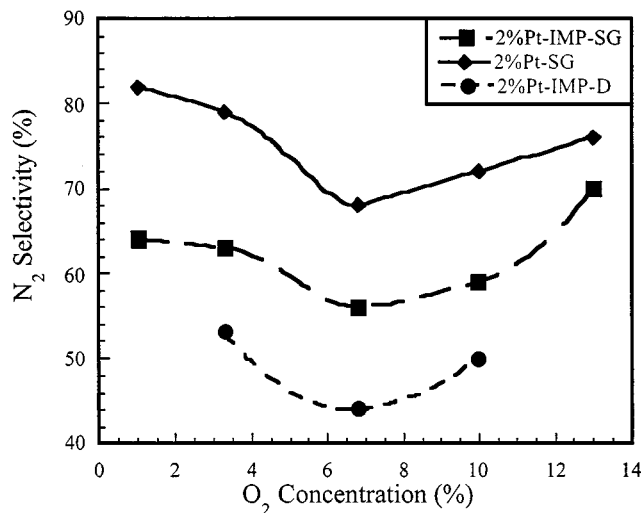
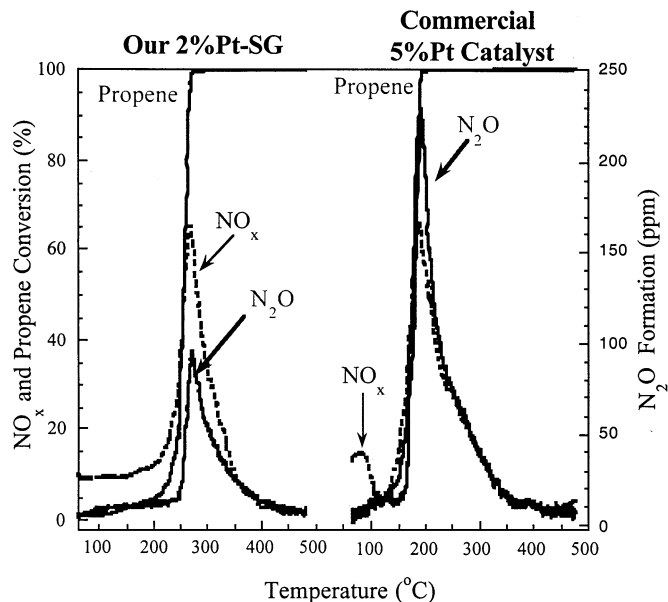


FIG. 7. Dependence of N<sub>2</sub> selectivity at peak NO<sub>x</sub> conversion on oxygen concentration. Conditions: 0.036 g catalyst, 750 ppm of NO 10 ppm NO<sub>2</sub>, 762 ppm C<sub>3</sub>H<sub>6</sub>, 2.6% H<sub>2</sub>O, varying oxygen concentration, remainder He. Total flow rate 72 ml/min.



**FIG. 8.**  $\text{NO}_x$  conversion activity and  $\text{N}_2\text{O}$  production of a 5% Pt/commercial alumina catalyst and a 2% Pt/alumina sol-gel (SG) catalyst during a temperature ramp experiment. Conditions: 1.0 g catalyst, 500 ppm  $\text{NO}_x$ , 1333 ppm  $\text{C}_3\text{H}_6$ , (+20 ppm  $\text{SO}_2$  for the SG catalyst), 10%  $\text{O}_2$  remainder  $\text{N}_2$  and 4000 ml/min of total flow rate.

feed also had 20 ppm  $\text{SO}_2$ ). One gram of catalyst was loaded into a quartz tubular reactor and the temperature of the reactor was ramped up from 50 to 600°C at the rate of 10°C/min. During the temperature ramp  $\text{NO}_x$  conversion,  $\text{N}_2\text{O}$  conversion and propene conversion were all measured with one second time resolution in real time. Figure 8 shows the results. Since the surfaces of both catalysts were clean at the beginning, there was significant adsorption of  $\text{NO}_x$  between 50 and 150°C seen in the form of a sharp peak at 50°C for both catalysts and a large bump between 60 and 130°C for the 5% Pt catalyst. The sol-gel catalyst does not have the bump and as a result appears to adsorb less  $\text{NO}_x$ . The peak  $\text{NO}_x$  conversions of both catalysts are comparable at ~65%, however, there is a big difference in the selectivities. At the peak of  $\text{NO}_x$  conversion, 5% Pt/alumina impregnation catalyst produces ~230 ppm of  $\text{N}_2\text{O}$ , more than 2.5 times the amount produced by the 2% Pt sol-gel catalyst, ~90 ppm. If we convert the observed concentrations to instantaneous selectivities we see that 230 ppm of  $\text{N}_2\text{O}$  would correspond to 40% more  $\text{NO}_x$  reduced than is possible with the 325 ppm of  $\text{NO}_x$  reduced at peak conversion.  $\text{N}_2\text{O}$  90 ppm produced by the sol-gel catalyst corresponds to an instantaneous  $\text{N}_2\text{O}$  selectivity of 54%, again worse than the steady state  $\text{N}_2\text{O}$  selectivity of ~28% observed with this catalyst in the presence of 10% oxygen as shown in Fig. 7. These high levels of  $\text{N}_2\text{O}$  are due to conversion of  $\text{NO}$  adsorbed at low temperatures to  $\text{N}_2\text{O}$  after the catalyst light off. The peak conversion temperatures are 200°C for the 5% Pt catalyst and 260°C for the 2% Pt sol-gel cata-

lyst. These values are in essential agreement with the steady state values measured in the microreactor.

#### D. Propene Combustion

As mentioned previously for all of our SCR experiments propene combustion was measured simultaneously with  $\text{NO}_x$  reduction. The data was not included in the figures showing  $\text{NO}_x$  reduction activity for clarity. However, in terms of the relationship between propene combustion and  $\text{NO}_x$  reduction, our observations are in agreement with the previous observations (11).  $\text{NO}_x$  reduction activity of the catalysts starts after propene combustion lights off and at the peak of  $\text{NO}_x$  conversion combustion of propene is ~95–98% complete. Water had no effect on the light off temperature of propene in the presence or absence of  $\text{NO}_x$  for all three types of catalysts. However, adding only 750 ppm of  $\text{NO}_x$  to the feed stream raised the light off temperature of propene from ~150 to ~210°C, an increase of 60°C in agreement with previous observations. Increased  $\text{O}_2$  in the feed lowered the light off temperature of propene, resulting in lowering the temperature for  $\text{NO}_x$  reduction activity by a comparable amount.

#### E. Long Term and High Temperature Stability and Resistance to $\text{SO}_2$

While diesel engine exhausts are not as demanding as the gasoline engine exhausts in terms of temperature stability, it is necessary that the  $\text{NO}_x$  reduction catalysts be able to survive several hours at 600–700°C (18). We exposed our 2% Pt-SG catalyst to three types of robustness tests: time on stream, extended exposure to  $\text{SO}_2$ , and high temperature treatment. The time on stream test consisted of leaving the catalyst on stream 10–20 h at a time for about 1500 h total (roughly equal to 50,000–100,000 miles of driving). During this period the feed concentrations of  $\text{NO}_x$  and propene were kept constant at ~750 ppm but the oxygen concentration was varied between 3 and 14%, and the temperature varied between 150 and 500°C. For several weeks of the test period we also included 25 ppm of  $\text{SO}_2$  in the feed. Figure 9 shows the results of these tests. The first point to note in Fig. 9 is that  $\text{SO}_2$  has no negative effect on the performance of the catalyst. Indeed the presence of  $\text{SO}_2$  along with the high oxygen concentration reduces the  $\text{N}_2\text{O}$  selectivity to below 10% for all conversions. If we compare Fig. 9 to Fig. 5 (the oxygen concentration and  $\text{NO}$  and propene concentrations are slightly higher in Fig. 9) we also see that there has been no decrease in the performance of the catalyst after one year of use, indeed the activities and selectivities have improved with time on stream. Figure 10 compares the performance of a catalyst aged at 800°C for 20 h in the presence of water vapor to a catalyst that has not been exposed to temperatures higher than 600°C. The only major difference is a shift of ~20°C to higher temperatures in the peak activity temperature.

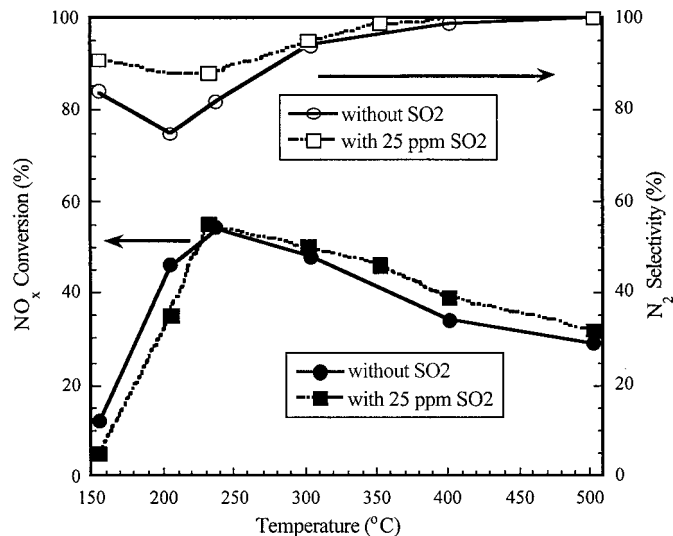


**FIG. 9.** NO<sub>x</sub> reduction activity of the 2% Pt/alumina SG catalyst, after extensive time on stream (~1500 h) and SO<sub>2</sub> exposure (~200 h). Conditions: 0.036 g catalyst, 1000 ppm of NO, 30 ppm NO<sub>2</sub>, 1000 ppm C<sub>3</sub>H<sub>6</sub>, 14% O<sub>2</sub>, 2.6% H<sub>2</sub>O and 25 ppm SO<sub>2</sub>, remainder He. Total flow rate 72 ml/min.

#### F. Effect of Water Vapor

While most of our studies were made with 2.6% water vapor in the feed, we also investigated the effect of water on activity and selectivity. We observed that the presence of water vapor did not change the N<sub>2</sub> selectivity of the SG cat-

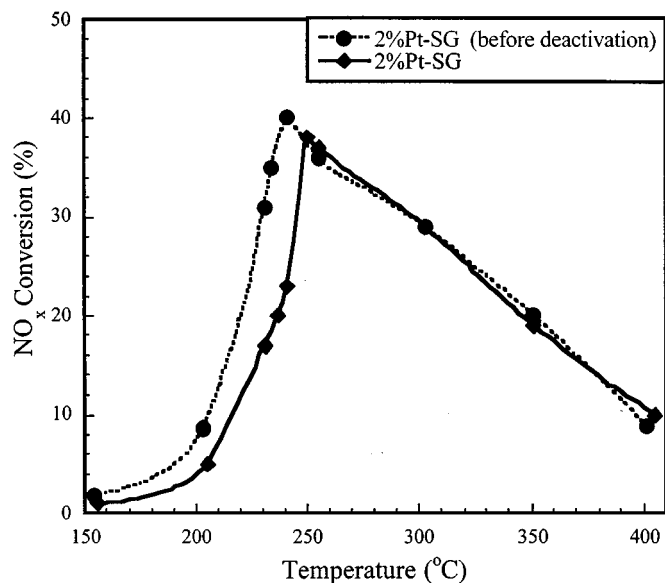


**FIG. 10.** A comparison of the NO<sub>x</sub> reduction activity of fresh 2% Pt-SG catalyst and deactivated 2% Pt-SG catalyst. Reaction conditions: 0.036 g catalyst, 600 ppm of NO, 10 ppm NO<sub>2</sub>, 600 ppm C<sub>3</sub>H<sub>6</sub>, 6% O<sub>2</sub>, 2.6% H<sub>2</sub>O, remainder He. Total flow rate 72 ml/min. Deactivation conditions: 0.036 g catalyst, 20% O<sub>2</sub> and 3% H<sub>2</sub>O, remainder He. The catalyst was kept at 800°C for 20 h. Total flow rate 72 ml/min.

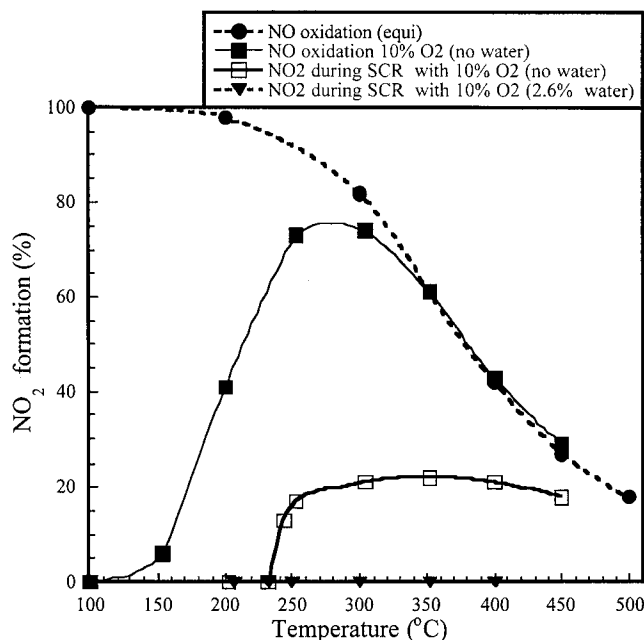


**FIG. 11.** Conversion of NO to NO<sub>2</sub> over the 2% Pt SG catalyst. The dashed line represents % conversion to NO<sub>2</sub> calculated from thermodynamic equilibrium data. Conditions: 0.036 g catalyst, 750 ppm of NO 10 ppm NO<sub>2</sub>, 762 ppm C<sub>3</sub>H<sub>6</sub>, 2.6% H<sub>2</sub>O, 10% O<sub>2</sub>, remainder He. Total flow rate 72 ml/min.

alyst at all but it increased the activity of the catalyst significantly on the high temperature side of the NO<sub>x</sub> conversion peak (broadened the activity window by ~50°C) and thus had a beneficial effect. Similar results were observed for the other two catalysts. We did not observe any effect of water on conversion or selectivity on the low temperature side.

#### G. NO Oxidation to NO<sub>2</sub>

Figure 11 shows NO<sub>2</sub> formation over the 2% Pt SG catalyst. In the absence of propene, NO is easily oxidized to NO<sub>2</sub> at significant rates starting at  $T = 150^\circ\text{C}$  and reaches its equilibrium limited value of ~75% conversion at around 300°C. When there is propene in the feed, however, NO<sub>2</sub> formation is drastically suppressed and NO<sub>2</sub> is seen only after 230°C. The amount of NO<sub>2</sub> produced during SCR was found to be a function of oxygen concentration as well as whether there was water in the feed or not. Lower oxygen concentrations led to higher NO to NO<sub>2</sub> conversions on the high temperature side of the peak NO<sub>x</sub> conversion. We observed that for the three 2% Pt catalysts the amount of NO<sub>2</sub> produced correlated with their selectivity to N<sub>2</sub>O. The SG catalyst had the least amount of NO<sub>2</sub> produced and the IMP-D catalyst had the most amount of NO<sub>2</sub> produced. In the presence of 2.6% water and 10% or more oxygen in the feed, the SG catalyst produced no NO<sub>2</sub> at all temperatures. The impregnation catalysts stopped producing NO<sub>2</sub> only when the oxygen concentration reached 13%.

**TABLE 1**  
**Physical Characteristics of the Catalysts**

Catalyst	1% Pt-SG	2% Pt-SG	2% Pt-Al <sub>2</sub> O <sub>3</sub> -SG	2% Pt-Al <sub>2</sub> O <sub>3</sub> -D
Surface area (m <sup>2</sup> /g)	303	274	314	95
Average pore diameter (Å)	74	68	77	196
% pore in the range of 10–100 Å	99	99	99	5
% of pore in 20 Å range around max.	81	85	62	41
Pt crystallite size, nm, determined with XRD	16	16	<5	33
Pt dispersion, (%), determined with CO chemisorption	N/A	10	51	7.5

### H. Catalyst Characterization

We characterized the catalysts with BET, XRD, TEM, and CO chemisorption. Table 1 gives the BET surface areas and pore sizes, distribution of pores and crystallite sizes, as well as dispersion of the catalysts. The sol–gel synthesis and calcination treatment we use produces Pt-alumina catalysts with BET surface areas of  $\sim 300$  m<sup>2</sup>/g and a narrow pore size distribution centered at  $d \sim 70$  Å. In comparison, the surface area of the Degussa  $\delta$ -alumina is only 95 m<sup>2</sup>/g and it has a rather large average pore size,  $d \sim 196$  Å, with a pore size distribution much broader than the other two catalysts. It is also interesting to note that the crystallite size of the 1% Pt SG catalyst is the same as the crystallite size of the 2% Pt SG catalyst. If we assume that the metallic colloidal Pt crystallites are formed during the gelation phase long before the alumina matrix solidifies, then it is possible to explain the observations. The size of the colloidal Pt particles formed through reduction of Pt precursor by the alcohols and the organic solvent at 85°C depends only on the solution conditions, which do not change with Pt loading thus we end up having loading independent Pt crystallite size. Since the particles are formed before alumina gel solidifies, it is possible to have them incorporated into the alumina matrix with much smaller average pore size. The dispersions of the 2% Pt catalysts obtained by CO chemisorption are in good agreement with dispersions estimated from the crystallite size measurements. This agreement shows that even though the Pt crystallite is caged in by the alumina support during the single-step sol–gel synthesis, most of the surface is still accessible from the gas phase.

Table 2 presents the performance of the catalysts in terms of turnover frequencies (TOFs). The low dispersion catalysts have higher TOFs as expected. In calculating NO decomposition TOFs we assumed that NO was reduced by first decomposing to N + O and obtained the TOFs by multiplying the moles of N<sub>2</sub> formed by two and adding to the moles of N<sub>2</sub>O formed. This table also shows the relative rates of N<sub>2</sub> and N<sub>2</sub>O formation at 250 and 200°C. Within error all three catalysts appear to have a ratio of  $\sim 3$  for N<sub>2</sub> formation. However, the N<sub>2</sub>O formation ratios are clearly different between the high dispersion catalyst ( $\sim 2.4$ ) and the low dispersion catalysts ( $\sim 6$  and 7.4). This implies that

perhaps there are different rate determining steps for N<sub>2</sub>O formation between the high and low dispersion catalysts.

Figure 12 shows the XRD spectra of 2% Pt loading catalysts as a function of catalyst preparation method. For the SG catalyst we see Pt peaks at  $2\theta$  of  $\sim 40$ ,  $\sim 46$ , and  $\sim 67.5$  degrees superimposed on alumina peaks ( $\gamma$  and  $\eta$ ) at  $\sim 39$ ,  $\sim 45.5$ , and  $\sim 66.8^\circ$ . For the IMP-D catalyst all of the Pt peaks are present and the alumina peaks match those of  $\delta$ -alumina exactly. The spectrum of the IMP-SG catalyst matches exactly that of the pure alumina made by the same sol–gel process. Absence of any detectable Pt crystallite peaks indicates that the average crystallite size in this catalyst is below the detection level by XRD ( $d \leq 3$ –5 nm). The alumina peaks seen with the pure sol–gel alumina match that of a mixture of  $\gamma$  and  $\eta$  aluminas. For the SG catalysts, approximate Pt crystallite size obtained by the Debye–Scherer equation from the broadening of the Pt (111) peak is  $16 \pm 1$  nm and was independent of Pt loading for the 3 samples we tested 1, 2, 5 wt% Pt within experimental error. The crystallite size obtained by the same method for the 2% Pt  $\delta$ -alumina impregnation catalyst is  $33 \pm 3$  nm. One of the interesting observations we have made with the XRD spectra of SG catalysts and are unable to explain the reasons for

**TABLE 2**  
**Comparison of the Turnover Frequencies for the Three 2% Pt Catalysts**

Catalyst and peak conversion temperature (°C)	SG 240	IMP-SG 225	IMP-D 250
Conversion (%)	46	58	39
N <sub>2</sub> selectivity (%)	69	56	43
NO <sub>x</sub> conversion TOF ( $\times 10^{-2}$ s <sup>-1</sup> )	5.15	1.27	5.82
NO decomposition TOF ( $\times 10^{-2}$ s <sup>-1</sup> )	4.32	0.99	4.19
N <sub>2</sub> O formation TOF ( $\times 10^{-2}$ s <sup>-1</sup> )	1.65	0.56	2.46
N <sub>2</sub> formation TOF ( $\times 10^{-2}$ s <sup>-1</sup> )	1.75	0.36	1.22
N <sub>2</sub> (250)/N <sub>2</sub> (200)	3.09	2.86	3.27
N <sub>2</sub> O(250)/N <sub>2</sub> O(200)	6.05	2.39	7.39

*Note.* Conditions are: 0.036 g of catalyst, 72 ml/min gas flow of composition 760 ppm NO + 10 ppm NO<sub>2</sub>, 750 ppm C<sub>3</sub>H<sub>6</sub>, 6.8% O<sub>2</sub>, remainder helium.

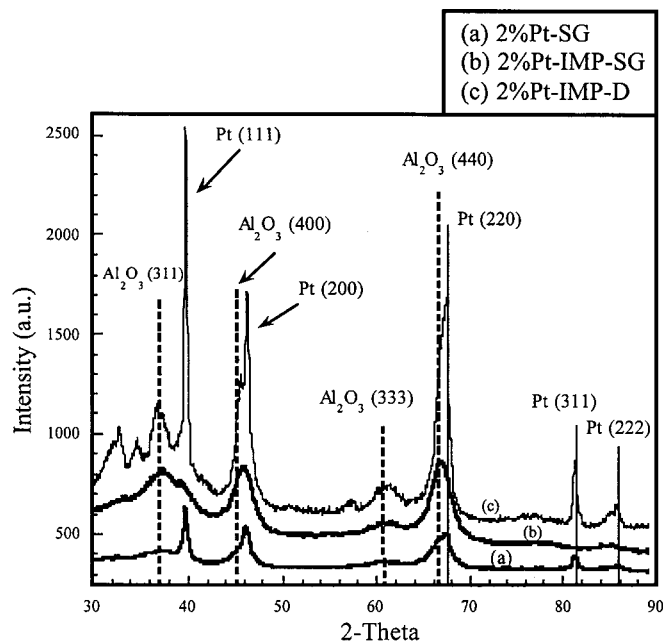


FIG. 12. XRD spectra of 2% Pt/alumina catalysts.

at this point, is that the relative intensity of the higher index planes increase with increasing Pt loading.

Because of the sensitivity of XRD analysis only to crystallites larger than 5 nm, we also used TEM to determine the average crystallite sizes of the SG and IMP-SG catalysts. Figure 13 shows the crystallite size distribution of the 2% Pt SG catalyst based on a sample of 200 Pt crystallite pictures. The distribution appears to have two very close peaks with 34% of the crystallites counted having a size of  $13 \pm 2$

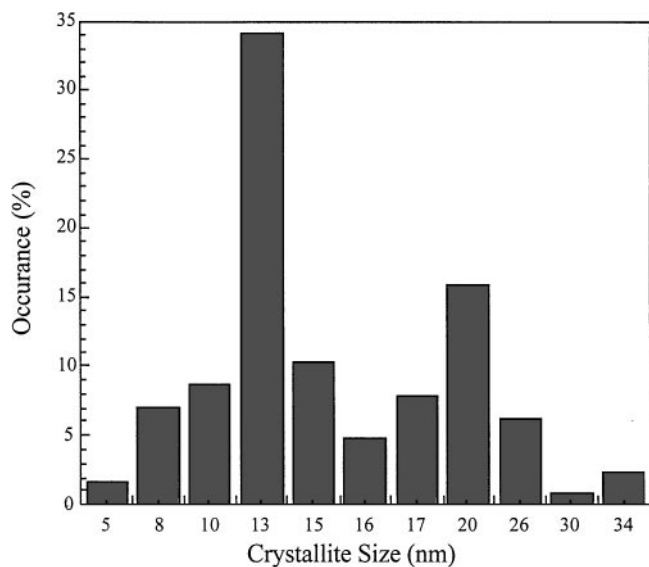


FIG. 13. Crystallite size distribution of 2% Pt single-step sol-gel catalyst (SG) obtained by TEM.

nm and 16% having a size of  $20 \pm 7$  nm. The average of this distribution also comes to  $15.5 \pm 6$  nm in excellent agreement with the XRD results. TEM measurements made with a sensitivity limit of 2 nm did not show any detectable Pt crystallites in the 2% Pt IMP-SG catalyst. However, elemental analysis of the imaged areas by energy dispersive X-ray emission spectroscopy (EDAX) showed the presence of Pt.

### III. DISCUSSION

#### A. Activity

One of the challenging questions to answer about Pt/alumina catalysts is the very weak dependence of the peak activity and N<sub>2</sub> selectivity for NO<sub>x</sub> reduction with propene on surface area and/or Pt loading. The three types of catalysts we tested extensively have the same metal loading but vastly different dispersions and crystallite sizes as seen in Table 1.

Currently there are three mechanisms that are proposed to explain the selective reduction of NO by alkenes over alumina and silica supported Pt catalysts. The first mechanism is that of oxidation of NO to NO<sub>2</sub> and then addition of NO<sub>2</sub> to propene followed by the decomposition of the nitrogen containing organic intermediates to give N<sub>2</sub> and N<sub>2</sub>O (19, 20). The second mechanism invokes a surface isocyanate or cyanide species (21). The third mechanism is a redox mechanism and involves dissociative adsorption of NO on metallic Pt sites (most likely edge and defect sites) to give N + O atoms. Surface N atoms recombine to give N<sub>2</sub>. Reaction of surface N with molecularly adsorbed NO results in N<sub>2</sub>O (11, 22). Surface O atoms are removed by reaction with the hydrocarbon intermediates on the surface completing the redox cycle and regenerating the metallic site. Support for the third mechanism comes from high vacuum studies. Single-crystal studies of Wang *et al.* (23), Xu and Ng (24), Gohndrone and Masel (25), and Masel (26) show that on noble metal surfaces NO adsorbs both molecularly and dissociatively and that the dissociation reaction is structure sensitive. N<sub>2</sub>O formation is observed as a result of N + NO reaction even at temperatures much below ambient (23). The same studies also show that NO decomposition is inhibited by the presence of oxygen (11, 24).

Our experimental observations with respect to NO<sub>x</sub> conversion activity and N<sub>2</sub> selectivity can be adequately explained by the third model and the finding by Burch *et al.* (27) and Jen and Otto (28) that in the presence of gas phase propene the Pt surface is mostly covered by carbonaceous species. On the metallic sites NO decomposition competes with O<sub>2</sub> decomposition. The atomic oxygen thus generated is removed by reaction with the carbonaceous surface species. At low temperatures the rate of NO decomposition is limited by the availability of metallic surface sites for decomposition because of blockage by carbonaceous



species. The rate of oxygen adsorption increases faster with temperature than the rate of NO adsorption and more of the hydrocarbon fragments are removed by reaction with atomic oxygen. This process opens up metallic surface sites leading to an increase in the rate of NO adsorption and dissociation with temperature as well as increased selectivity towards  $N_2O$ . As the surface coverage of oxygen increases further with temperature dissociative adsorption of NO is suppressed (24) decreasing the reduction rate. Thus the temperature at which the maximum in NO reduction is reached as well as the percent conversion of NO is determined by the relative activation energies of NO decomposition versus  $O_2$  decomposition and propene combustion. A peak in activity and a minimum in selectivity results because at the peak there is a balance between the carbonaceous species removal rate and surface oxidation. This results in a maximum in the concentration of sites over which NO can decompose as well as adsorb molecularly. Increased molecularly adsorbed NO concentration leads to higher rates of  $N_2O$  formation and thus the minimum in selectivity. At temperatures above the peak temperature, surface concentration of molecularly adsorbed NO continues to decrease due to a combination of lower sticking coefficients as well as decreased availability of sites. Increasing oxygen concentration simply lowers the temperature at which oxygen competes successfully with NO for adsorption and removal of carbonaceous species. Thus increased oxygen concentration should result in broadening of the temperature window on the low temperature side of the peak conversion, in agreement with the experimental observations.

With this mechanism the only way to increase NO conversion is through increasing the number of sites on which NO decomposition takes place. NO decomposition is structure sensitive (26) and requires an ensemble of metallic atoms to take place. This is more likely on larger metallic crystallites than smaller crystallites, thus the increased TOFs observed for the low dispersion catalysts which result in relatively small decreases in conversion compared to the decrease in surface area.

### B. Selectivity

If we assume that NO decomposition is the primary route to selective NO reduction then the  $N_2$  selectivity is a function of the relative surface concentrations of molecularly adsorbed NO and atomic N.  $N_2$  selectivity will increase if the dissociation rate of NO increases and/or the surface concentration of NO decreases. Since there is ample evidence from single-crystal studies that dissociation of NO is structure sensitive (23–26) dissociation rate should be a function of preparation method and crystallite size. Table 2 compares the NO decomposition turnover numbers for the three different catalysts. The single-step sol-gel catalysts have the highest TOFs, evidence that their preparation method results in more exposed high index planes

and/or defects over which NO decomposes. However, the TOF for the IMP-D catalyst is not much smaller, indicating a similar concentration of decomposition sites. The large difference in selectivity can then only be explained by a lower surface concentration of molecular NO. This also explains the higher selectivities we observe in comparison to the previous investigators under similar operating conditions (2, 16, 29). Since molecularly adsorbed NO competes with hydrocarbon fragments and possibly with oxygen increasing the concentration of oxygen and hydrocarbon on the catalyst surface should also lead to higher  $N_2$  selectivity. Figure 7 shows the increase in  $N_2$  selectivity with increased oxygen concentration above 6.8% oxygen in the feed. According to the redox model, increasing surface concentration of hydrocarbons should also lead to higher  $N_2$  selectivities. Using a hydrocarbon to NO ratio much higher (14 C to 1 NO) than the generally used 3 to 1 ratio, Burch and Ottery (13) have also reported  $N_2$  selectivities as high as 100% (toluene) and 66% (propene) on Pt/alumina catalysts. The changes in selectivity due to lower surface concentrations of NO is also supported by the  $NO_2$  formation data. As shown in Fig. 11  $NO_2$  formation on the sol-gel catalyst is completely suppressed at all temperatures in the presence of 10%  $O_2$  and 2.6% water. Complete suppression over the impregnation catalysts require higher concentrations of oxygen and/or water.

Xu and Goodman (30) observed that Pd crystallites less than 5 nm in size have 100% selectivity to  $N_2$  this is not the case for our IMP-SG catalyst which has an average crystallite size less than  $\sim 3$  nm. Thus Pt appears to behave differently than Pd. This may be due to the ease of reduction of Pt versus Pd.

## V. CONCLUSIONS

Our results show that for selective  $NO_x$  reduction with propene over Pt/alumina catalysts:

1. The single-step sol-gel preparation method gives active and the most  $N_2$  selective Pt/alumina catalysts. These catalysts are highly resistant to sintering and  $SO_2$  poisoning. The activities of the sol-gel catalysts improve with time on stream rather than decaying.
2. Single-step sol-gel preparation method produces quite narrowly distributed Pt crystallites whose size is determined before the alumina support is formed.
3. Pt/alumina catalysts show their worst  $N_2$  selectivity with 5–7%  $O_2$  concentration. At lower or higher oxygen concentrations the  $N_2$  selectivity is better.
4. Increasing the oxygen content of the feed all the way to 13% increases the, FWHM, of Pt/alumina catalysts almost to  $\sim 200^\circ C$ , which results in significant  $NO_x$  reduction activity even at  $450^\circ C$  with the sol-gel catalysts.
5. Inclusion of water vapor in the feed and oxygen concentrations higher than 10% completely suppress  $NO_2$

formation over the Pt/alumina catalysts as well as improve the selective reduction performance at temperatures above the peak conversion temperature.

### ACKNOWLEDGMENTS

Partial financial support of this research by a National Science Foundation Grant NSF-CTS-9872112 and Ford Motor Company is gratefully acknowledged. We are grateful to Professor L. T. Thompson for the use of his group's BET surface area analyzer and to Mr. John Cavataio for the temperature programmed reaction experiment and CO chemisorption experiments.

### REFERENCES

1. Hamada, H., Kintaichi, Y., Sasaki, M., Ito, T., and Tabata, M., *Appl. Catal.* **75**, L1 (1991).
2. Obuchi, A., Ohi, A., Nakamura, M., Ogata, A., Mizuno, K., and Ohuchi, H., *Appl. Catal. B: Environmental* **2**, 71 (1993).
3. Hamada, H., Kintaichi, Y., Sasaki, M., Ito, T., and Tabata, M., *Appl. Catal. A: General* **88**, L1 (1992).
4. Guyon, M., Le Chanu, V., Gilot, P., Kessler, H., and Prado, G., *Appl. Catal. B: Environmental* **8**, 183 (1996).
5. Guo, J., Konno, M., Chikahisa, T., Murayama, T., and Iwamoto, M., *JSAE Rev.* **16**, 21 (1995).
6. Armor, N. J., and Farris, S. T., *Appl. Catal. B: Environmental* **4**, L11 (1994).
7. Kharas, K. C. C., Robota, K. J., and Liu, D. J., *Appl. Catal. B: Environmental* **2**, 225 (1993).
8. Petunchi, O. J., and Hall, W. K., *Appl. Catal. B: Environmental* **3**, 239 (1994).
9. Sasaki, M., Hamada, H., Kintaichi, Y., Ito, Y., and Tabata, M., *Catal. Lett.* **15**, 297 (1992).
10. Burch, R., Millington, P. J., and Walker, A. P., *Appl. Catal. B: Environmental* **4**, 65 (1994).
11. Burch, R., and Millington, P. J., *Catal. Today* **26**, 185 (1995).
12. Amiridis, M. D., Pereira, C. J., and Roberts, K. L., *Appl. Catal. B: Environmental* **14**, 203 (1997).
13. Burch, R., and Ottery, D., *Appl. Catal. B: Environmental* **13**, 105 (1997).
14. Seker, E., Cavataio, J., Gulari, E., Lorphongpaiboon, P., and Osuwan, S., *Appl. Catal. A: General* **183**, 121 (1999).
15. Seker, E., and Gulari, E., *J. Catal.* **179**, 339 (1998).
16. Burch, R., and Watling, T. C., *Appl. Catal. B: Environmental* **11**, 207 (1997).
17. McCabe, R., private communication.
18. Private communication from Dr. R. Hammerle, Ford Motor Co., 1999.
19. Tanaka, T., Okuhara, T., and Misono, M., *Appl. Catal. B: Environmental* **4**, L1 (1994).
20. Jayat, F., Lembacher, C., Schubert, U., and Martens, J. A., *Appl. Catal. B: Environmental* **21**, 221 (1999).
21. Captain, D. K., Roberts, K. L., and Amiridis, M. D., *Catal. Today* **42**, 93 (1998).
22. Engler, B. H., Leyrer, J., Lox, E. S., and Ostgathe, K., in "Catalysis and Automotive Pollution Control III" (A. Frennet and J. M. Bastin, Eds.), Vol. 96, p. 529. Elsevier, Amsterdam, 1995.
23. Wang, H., Tobin, R. G., Dimaggio, C. L., Fisher, G. B., and Lambert, D. K., *J. Chem. Phys.* **107**, 22 (1997).
24. Xu, H., and Simon Ng, K. Y., *Surf. Sci.* **365**, 779 (1996).
25. Gohndrone, J. M., and Masel, R. I., *Surf. Sci.* **209**, 44 (1989).
26. Masel, R. I., *Catal. Rev. Sci. Eng.* **28**, 335 (1986).
27. Burch, R., and Watling, T. C., *Catal. Lett.* **43**, 19 (1997).
28. Jen, H. W., and Otto, K., *Catal. Lett.* **26**, 217 (1994).
29. Burch, R., and Watling, T. C., *Appl. Catal. B: Environmental* **17**, 131 (1998).
30. Xu, X., and Goodman, D. W., *Catal. Lett.* **24**, 31 (1994).